

Towards unification of quark and lepton flavors in A_4 modular invariance

Hiroshi Okada ^{a,b*} and Morimitsu Tanimoto ^{c†}

^a*Asia Pacific Center for Theoretical Physics, Pohang 37673, Republic of Korea*

^b*Department of Physics, Pohang University of Science and Technology, Pohang 37673, Republic of Korea*

^c*Department of Physics, Niigata University, Niigata 950-2181, Japan*

Abstract

We study quark and lepton mass matrices in the A_4 modular symmetry towards the unification of the quark and lepton flavors. We adopt modular forms of weights 2 and 6 for the quarks and charged leptons while we use modular forms of weight 4 for the neutrino mass matrix generated by the Weinberg operator. The modulus τ is common in both quark and lepton mass matrices. We obtain the successful quark mass matrices, in which the down-type quark mass matrix is constructed by modular forms of weight 2, but the up-type quark mass matrix is constructed by modular forms of weight 6. Supposing that the charged lepton mass matrix is constructed by modular forms of weight 6, predicted lepton mixing angles are consistent with observed ones for the normal hierarchy of neutrino masses. The effective neutrino mass of the $0\nu\beta\beta$ decay is $\langle m_{ee} \rangle = 5\text{--}12\text{meV}$ and $19\text{--}24\text{meV}$. The sum of neutrino masses is $102\text{--}107\text{meV}$. It is remarked that the modulus τ is fixed around $\tau = i$ in the fundamental region of $\text{SL}(2, Z)$, which suggests the residual symmetry Z_2 in the quark and lepton mass matrices. On the other hand, the inverted hierarchy of neutrino masses is excluded by the observed upper bound of the sum of neutrino masses.

*E-mail address: hiroshi.okada@apctp.org

†E-mail address: tanimoto@muse.sc.niigata-u.ac.jp

1 Introduction

The standard model (SM) was well established by the discovery of the Higgs boson. However, the flavor theory of quarks and leptons is still unknown. In order to understand the origin of the flavor structure, many works have appeared by using the discrete groups for flavors. In the early models of quark masses and mixing angles, the S_3 symmetry was used [1, 2]. It was also discussed to understand the large mixing angle [3] in the oscillation of atmospheric neutrinos [4]. For the last twenty years, the discrete symmetries of flavors have been developed, that is motivated by the precise observation of flavor mixing angles of leptons [5–13].

Many models have been proposed by using the non-Abelian discrete groups S_3 , A_4 , S_4 , A_5 and other groups with larger orders to explain the large neutrino mixing angles. Among them, the A_4 flavor model is attractive one because the A_4 group is the minimal one including a triplet irreducible representation, which allows for a natural explanation of the existence of three families of leptons [14–20]. However, variety of models is so wide that it is difficult to obtain a clear evidence of the A_4 flavor symmetry.

Recently, a new approach to the lepton flavor problem appeared based on the invariance under the modular group [21], where the model of the finite modular group $\Gamma_3 \simeq A_4$ has been presented. This work inspired further studies of the modular invariance to the lepton flavor problem. It should be emphasized that there is a significant difference between the models based on the A_4 modular symmetry and those based on the usual non-Abelian discrete A_4 flavor symmetry. Yukawa couplings transform non-trivially under the modular group and are written in terms of modular forms which are holomorphic functions of a complex parameter, the modulus τ .

The modular group includes the finite groups S_3 , A_4 , S_4 , and A_5 [22]. Therefore, an interesting framework for the construction of flavor models has been put forward based on the $\Gamma_3 \simeq A_4$ modular group [21], and further, based on $\Gamma_2 \simeq S_3$ [23]. The proposed flavor models with modular symmetries $\Gamma_4 \simeq S_4$ [24] and $\Gamma_5 \simeq A_5$ [25] have also stimulated studies of flavor structures of quarks and leptons. Phenomenological discussions of the neutrino flavor mixing have been done based on A_4 [26, 27], S_4 [28, 29], A_5 [30], and T' [31] modular groups, respectively. In particular, the comprehensive analysis of the A_4 modular group has provided a distinct prediction of the neutrino mixing angles and the CP violating phase [27]. The A_4 modular symmetry has been also applied to the $SU(5)$ grand unified theory (GUT) of quarks and leptons [32], while the residual symmetry of the A_4 modular symmetry has been investigated phenomenologically [33]. Furthermore, modular forms for $\Delta(96)$ and $\Delta(384)$ were constructed [34], and the extension of the traditional flavor group is discussed with modular symmetries [35]. Moreover, multiple modular symmetries are proposed as the origin of flavor [36]. The modular invariance has been also studied combining with the generalized CP symmetries for theories of flavors [37]. The quark mass matrix has been discussed in the S_3 and A_4 modular symmetries as well [38–40]. Besides mass matrices of quarks and leptons, related topics have been discussed in the baryon number violation [38], the dark matter [41, 42] and the modular symmetry anomaly [43].

In this work, we study both quarks and leptons in the A_4 modular symmetry. If the flavor of quarks and leptons is originated from a same two-dimensional compact space, the quarks and leptons have same flavor symmetry and the same value of the modulus τ . Therefore, it is challenging to reproduce observed hierarchical three Cabibbo-Kobayashi-Maskawa (CKM) mixing angles and the CP violating phase while observed large mixing angles are also reproduced in the lepton sector within the framework of the A_4 modular invariance with the common τ . This work provides a

new aspect in order to discover the unification theory of the quark and lepton flavors. We have already discussed the quark mass matrices in terms of A_4 modular forms of weight 2. It has been found that quark mass matrices of A_4 do not work unless Higgs sector is extended to the A_4 triplet representation. In this paper, we propose to adopt modular forms of weight 6 in addition to modular ones of weight 2 for quarks with the Higgs sector of SM. We also use modular forms of weight 4 for the neutrino mass matrix generated by the Weinberg operator. By taking the common value of modulus τ , we obtain the successful CKM mixing matrix and Pontecorvo-Maki-Nakagawa-Sakata (PMNS) matrix. Finally, we predict the CP violating Dirac phase of leptons, which is expected to be observed at T2K and NO ν A experiments [44, 45].

The paper is organized as follows. In section 2, we give a brief review on the modular symmetry and modular forms of weights 2, 4 and 6. In section 3, we present the model for quark mass matrices in the A_4 modular symmetry. In section 4, we show numerical results for the CKM matrix. In section 5, we discuss the lepton mass matrices and present numerical results. Section 6 is devoted to a summary. In Appendix A, the tensor product of the A_4 group is presented. In Appendix B, we show how to determine the coupling coefficients of quarks. In Appendix C, we present how to obtain Dirac CP phase, Majorana phases and effective mass of the $0\nu\beta\beta$ decay.

2 Modular group and modular forms of weights 2, 4, 6

The modular group $\bar{\Gamma}$ is the group of linear fractional transformation γ acting on the modulus τ , belonging to the upper-half complex plane as:

$$\tau \longrightarrow \gamma\tau = \frac{a\tau + b}{c\tau + d}, \quad \text{where } a, b, c, d \in \mathbb{Z} \text{ and } ad - bc = 1, \quad \text{Im}[\tau] > 0, \quad (1)$$

which is isomorphic to $PSL(2, \mathbb{Z}) = SL(2, \mathbb{Z})/\{I, -I\}$ transformation. This modular transformation is generated by S and T ,

$$S : \tau \longrightarrow -\frac{1}{\tau}, \quad T : \tau \longrightarrow \tau + 1, \quad (2)$$

which satisfy the following algebraic relations,

$$S^2 = \mathbb{I}, \quad (ST)^3 = \mathbb{I}. \quad (3)$$

We introduce the series of groups $\Gamma(N)$ ($N = 1, 2, 3, \dots$), called principal congruence subgroups, defined by

$$\Gamma(N) = \left\{ \begin{pmatrix} a & b \\ c & d \end{pmatrix} \in SL(2, \mathbb{Z}), \quad \begin{pmatrix} a & b \\ c & d \end{pmatrix} = \begin{pmatrix} 1 & 0 \\ 0 & 1 \end{pmatrix} \pmod{N} \right\}. \quad (4)$$

For $N = 2$, we define $\bar{\Gamma}(2) \equiv \Gamma(2)/\{I, -I\}$. Since the element $-I$ does not belong to $\Gamma(N)$ for $N > 2$, we have $\bar{\Gamma}(N) = \Gamma(N)$. The quotient groups defined as $\Gamma_N \equiv \bar{\Gamma}/\bar{\Gamma}(N)$ are finite modular groups. In this finite groups Γ_N , $T^N = \mathbb{I}$ is imposed. The groups Γ_N with $N = 2, 3, 4, 5$ are isomorphic to S_3 , A_4 , S_4 and A_5 , respectively [22].

Modular forms of level N are holomorphic functions $f(\tau)$ transforming under the action of $\Gamma(N)$ as:

$$f(\gamma\tau) = (c\tau + d)^k f(\tau), \quad \gamma \in \Gamma(N), \quad (5)$$

where k is the so-called as the modular weight.

Superstring theory on the torus T^2 or orbifold T^2/Z_N has the modular symmetry [46–51]. Its low energy effective field theory is described in terms of supergravity theory, and string-derived supergravity theory has also the modular symmetry. Under the modular transformation of Eq.(1), chiral superfields $\phi^{(I)}$ transform as [52],

$$\phi^{(I)} \rightarrow (c\tau + d)^{-k_I} \rho^{(I)}(\gamma) \phi^{(I)}, \quad (6)$$

where $-k_I$ is the modular weight and $\rho^{(I)}(\gamma)$ denotes an unitary representation matrix of $\gamma \in \Gamma(N)$.

In the present article we study global supersymmetric models, e.g., minimal supersymmetric extensions of the Standard Model (MSSM). The superpotential which is built from matter fields and modular forms is assumed to be modular invariant, i.e., to have a vanishing modular weight. For given modular forms this can be achieved by assigning appropriate weights to the matter superfields.

The kinetic terms are derived from a Kähler potential. The Kähler potential of chiral matter fields $\phi^{(I)}$ with the modular weight $-k_I$ is given simply by

$$K^{\text{matter}} = \frac{1}{[i(\bar{\tau} - \tau)]^{k_I}} |\phi^{(I)}|^2, \quad (7)$$

where the superfield and its scalar component are denoted by the same letter, and $\bar{\tau} = \tau^*$ after taking the vacuum expectation value (VEV). Therefore, the canonical form of the kinetic terms is obtained by the overall normalization of the quark/lepton mass matrices ¹.

For $\Gamma_3 \simeq A_4$, the dimension of the linear space $\mathcal{M}_k(\Gamma_3)$ of modular forms of weight k is $k + 1$ [54–56], i.e., there are three linearly independent modular forms of the lowest non-trivial weight 2. These forms have been explicitly obtained [21] in terms of the Dedekind eta-function $\eta(\tau)$:

$$\eta(\tau) = q^{1/24} \prod_{n=1}^{\infty} (1 - q^n), \quad q = \exp(i2\pi\tau), \quad (8)$$

where $\eta(\tau)$ is a so called modular form of weight 1/2. In what follows we will use the following basis of the A_4 generators S and T in the triplet representation:

$$S = \frac{1}{3} \begin{pmatrix} -1 & 2 & 2 \\ 2 & -1 & 2 \\ 2 & 2 & -1 \end{pmatrix}, \quad T = \begin{pmatrix} 1 & 0 & 0 \\ 0 & \omega & 0 \\ 0 & 0 & \omega^2 \end{pmatrix}, \quad (9)$$

where $\omega = \exp(i\frac{2}{3}\pi)$. The modular forms of weight 2, $\mathbf{Y}_3^{(2)} = (Y_1(\tau), Y_2(\tau), Y_3(\tau))^T$ transforming as a triplet of A_4 can be written in terms of $\eta(\tau)$ and its derivative [21]:

$$\begin{aligned} Y_1(\tau) &= \frac{i}{2\pi} \left(\frac{\eta'(\tau/3)}{\eta(\tau/3)} + \frac{\eta'((\tau+1)/3)}{\eta((\tau+1)/3)} + \frac{\eta'((\tau+2)/3)}{\eta((\tau+2)/3)} - \frac{27\eta'(3\tau)}{\eta(3\tau)} \right), \\ Y_2(\tau) &= \frac{-i}{\pi} \left(\frac{\eta'(\tau/3)}{\eta(\tau/3)} + \omega^2 \frac{\eta'((\tau+1)/3)}{\eta((\tau+1)/3)} + \omega \frac{\eta'((\tau+2)/3)}{\eta((\tau+2)/3)} \right), \\ Y_3(\tau) &= \frac{-i}{\pi} \left(\frac{\eta'(\tau/3)}{\eta(\tau/3)} + \omega \frac{\eta'((\tau+1)/3)}{\eta((\tau+1)/3)} + \omega^2 \frac{\eta'((\tau+2)/3)}{\eta((\tau+2)/3)} \right). \end{aligned} \quad (10)$$

¹The most general Kähler potential consistent with the modular symmetry possibly contains additional terms, as recently pointed out in Ref. [53]. However, we consider only the simplest form of the Kähler potential.

The overall coefficient in Eq. (10) is one possible choice. It cannot be uniquely determined. The triplet modular forms of weight 2 have the following q -expansions:

$$\mathbf{Y}_3^{(2)} = \begin{pmatrix} Y_1(\tau) \\ Y_2(\tau) \\ Y_3(\tau) \end{pmatrix} = \begin{pmatrix} 1 + 12q + 36q^2 + 12q^3 + \dots \\ -6q^{1/3}(1 + 7q + 8q^2 + \dots) \\ -18q^{2/3}(1 + 2q + 5q^2 + \dots) \end{pmatrix}. \quad (11)$$

They satisfy also the constraint [21]:

$$(Y_2(\tau))^2 + 2Y_1(\tau)Y_3(\tau) = 0. \quad (12)$$

The modular forms of the higher weight, k , can be obtained by the A_4 tensor products of the modular forms with weight 2, $\mathbf{Y}_3^{(2)}$, as given in Appendix A. For $k = 4$, there are five modular forms by the tensor product of $\mathbf{3} \otimes \mathbf{3}$ as:

$$\begin{aligned} \mathbf{Y}_1^{(4)} &= Y_1^2 + 2Y_2Y_3, \quad \mathbf{Y}_{1'}^{(4)} = Y_3^2 + 2Y_1Y_2, \quad \mathbf{Y}_{1''}^{(4)} = Y_2^2 + 2Y_1Y_3 = 0, \\ \mathbf{Y}_3^{(4)} &= \begin{pmatrix} Y_1^{(4)} \\ Y_2^{(4)} \\ Y_3^{(4)} \end{pmatrix} = \begin{pmatrix} Y_1^2 - Y_2Y_3 \\ Y_3^2 - Y_1Y_2 \\ Y_2^2 - Y_1Y_3 \end{pmatrix}, \end{aligned} \quad (13)$$

where $\mathbf{Y}_{1''}^{(4)}$ vanishes due to the constraint of Eq. (12). For $k = 6$, there are seven modular forms by the tensor products of A_4 as:

$$\begin{aligned} \mathbf{Y}_1^{(6)} &= Y_1^3 + Y_2^3 + Y_3^3 - 3Y_1Y_2Y_3, \\ \mathbf{Y}_3^{(6)} &\equiv \begin{pmatrix} Y_1^{(6)} \\ Y_2^{(6)} \\ Y_3^{(6)} \end{pmatrix} = \begin{pmatrix} Y_1^3 + 2Y_1Y_2Y_3 \\ Y_1^2Y_2 + 2Y_2^2Y_3 \\ Y_1^2Y_3 + 2Y_3^2Y_2 \end{pmatrix}, \quad \mathbf{Y}_{3'}^{(6)} \equiv \begin{pmatrix} Y_1'^{(6)} \\ Y_2'^{(6)} \\ Y_3'^{(6)} \end{pmatrix} = \begin{pmatrix} Y_3^3 + 2Y_1Y_2Y_3 \\ Y_3^2Y_1 + 2Y_1^2Y_2 \\ Y_3^2Y_2 + 2Y_2^2Y_1 \end{pmatrix}. \end{aligned} \quad (14)$$

By using these modular forms of weights 2, 4, 6, we discuss quark and lepton mass matrices.

3 Quark mass matrices in the A_4 modular invariance

Let us consider a A_4 modular invariant flavor model for quarks. There are freedoms for the assignments of irreducible representations and modular weights to quarks and Higgs doublets.

The simplest one is to assign the triplet of the A_4 group to three left-handed quarks, but three different singlets ($\mathbf{1}, \mathbf{1}', \mathbf{1}''$) of A_4 to the three right-handed quarks, (u^c, c^c, t^c) and (d^c, s^c, b^c) , respectively, where the sum of weights of the left-handed and the right-handed quarks is -2 .

Then, there appear three independent couplings in the superpotential of the up-type and down-type quark sectors, respectively, as follows:

$$w_u = \alpha_u u^c H_u \mathbf{Y}_3^{(2)} Q + \beta_u c^c H_u \mathbf{Y}_3^{(2)} Q + \gamma_u t^c H_u \mathbf{Y}_3^{(2)} Q, \quad (15)$$

$$w_d = \alpha_d d^c H_d \mathbf{Y}_3^{(2)} Q + \beta_d s^c H_d \mathbf{Y}_3^{(2)} Q + \gamma_d b^c H_d \mathbf{Y}_3^{(2)} Q, \quad (16)$$

where Q is the left-handed A_4 triplet quarks, and H_q is the Higgs doublets. The parameters $\alpha_q, \beta_q, \gamma_q$ ($q = u, d$) are constant coefficients. Assign the left-handed A_4 triplet Q to (t_L, c_L, u_L) and (b_L, s_L, d_L) ². By using the decomposition of the A_4 tensor product in Appendix A, the superpotentials in Eqs.(15) and (16) give the mass matrix of quarks, which is written in terms of modular forms of weight 2:

$$M_q = v_q \begin{pmatrix} \alpha_q & 0 & 0 \\ 0 & \beta_q & 0 \\ 0 & 0 & \gamma_q \end{pmatrix} \begin{pmatrix} Y_2 & Y_3 & Y_1 \\ Y_3 & Y_1 & Y_2 \\ Y_1 & Y_2 & Y_3 \end{pmatrix}_{RL}, \quad (q = u, d), \quad (17)$$

where τ of the modular forms $Y_i(\tau)$ is omitted. The coefficient v_q is the VEV of the Higgs field H_q . Unknown couplings $\alpha_q, \beta_q, \gamma_q$ can be adjusted to the observed quark masses. The remained parameter is only the modulus, τ . The numerical study of the quark mass matrix in Eq.(17) is rather easy. However, it is impossible to reproduce observed hierarchical three CKM mixing angles by fixing one complex parameter τ .

	Q	(q_1^c, q_2^c, q_3^c)	H_q	$\mathbf{Y}_3^{(6)}, \mathbf{Y}_{3'}^{(6)}$
$SU(2)$	2	1	2	1
A_4	3	(1, 1'', 1')	1	3, 3'
$-k_I$	-2	(-4, -4, -4)	0	$k = 6$

Table 1: Assignments of representations and weights $-k_I$ for MSSM fields and modular forms.

In order to present realistic quark mass matrices, we use modular forms of weight 6 in Eq.(14). Then, there appear six independent couplings in the superpotential of the quark sector as follows:

$$w_q = \alpha_q q_1^c H_q \mathbf{Y}_3^{(6)} Q + \alpha'_q q_1^c H_q \mathbf{Y}_{3'}^{(6)} Q + \beta_q q_2^c H_q \mathbf{Y}_3^{(6)} Q + \beta'_q q_2^c H_q \mathbf{Y}_{3'}^{(6)} Q + \gamma_q q_3^c H_q \mathbf{Y}_3^{(6)} Q + \gamma'_q q_3^c H_q \mathbf{Y}_{3'}^{(6)} Q, \quad (18)$$

where assignments of representations and weights for MSSM fields are given in Table 1. The quark mass matrix is written as:

$$M_q = \begin{pmatrix} \alpha_q & 0 & 0 \\ 0 & \beta_q & 0 \\ 0 & 0 & \gamma_q \end{pmatrix} \left[\begin{pmatrix} Y_2^{(6)} & Y_3^{(6)} & Y_1^{(6)} \\ Y_3^{(6)} & Y_1^{(6)} & Y_2^{(6)} \\ Y_1^{(6)} & Y_2^{(6)} & Y_3^{(6)} \end{pmatrix} + \begin{pmatrix} g_{q1} & 0 & 0 \\ 0 & g_{q2} & 0 \\ 0 & 0 & g_{q3} \end{pmatrix} \begin{pmatrix} Y_2'^{(6)} & Y_3'^{(6)} & Y_1'^{(6)} \\ Y_3'^{(6)} & Y_1'^{(6)} & Y_2'^{(6)} \\ Y_1'^{(6)} & Y_2'^{(6)} & Y_3'^{(6)} \end{pmatrix} \right]_{RL}. \quad (19)$$

Parameters $\alpha_q, \beta_q, \gamma_q$ are real, on the other hand, g_{qi} ($i = 1, 2, 3$) are complex parameters. Since the number of extra parameters are larger than the number of the CKM observables, we scan parameters only in the direction of $g_{q1} = g_{q2} = g_{q3} \equiv g_q$ in our numerical studies. This condition corresponds to $\alpha'_q/\alpha_q = \beta'_q/\beta_q = \gamma'_q/\gamma_q$. Indeed, we have found parameter sets, which is consistent with the CKM observables, in our numerical results.

Let us consider three cases of mass matrices by using modular forms of weights 2 and 6.

Model-I : down-type quark mass matrix with $\mathbf{Y}_3^{(2)}$ and up-type one with $\mathbf{Y}_3^{(6)}$ and $\mathbf{Y}_{3'}^{(6)}$

²This assignment is different from the conventional one, (u_L, c_L, t_L) and (d_L, s_L, b_L) , which corresponds to the exchange between the first column and the third one in the quark matrices. It is found that our assignments are preferred in our phenomenological analysis. In general, there exist three rotations and three reflections of quarks, and these degrees of freedom are useful to get the CKM matrix consistent with observations.

$$M_d = v_d \begin{pmatrix} \alpha_d & 0 & 0 \\ 0 & \beta_d & 0 \\ 0 & 0 & \gamma_d \end{pmatrix} \begin{pmatrix} Y_2 & Y_3 & Y_1 \\ Y_3 & Y_1 & Y_2 \\ Y_1 & Y_2 & Y_3 \end{pmatrix}_{RL},$$

$$M_u = v_u \begin{pmatrix} \alpha_u & 0 & 0 \\ 0 & \beta_u & 0 \\ 0 & 0 & \gamma_u \end{pmatrix} \left[\begin{pmatrix} Y_2^{(6)} & Y_3^{(6)} & Y_1^{(6)} \\ Y_3^{(6)} & Y_1^{(6)} & Y_2^{(6)} \\ Y_1^{(6)} & Y_2^{(6)} & Y_3^{(6)} \end{pmatrix} + g_u \begin{pmatrix} Y_2'^{(6)} & Y_3'^{(6)} & Y_1'^{(6)} \\ Y_3'^{(6)} & Y_1'^{(6)} & Y_2'^{(6)} \\ Y_1'^{(6)} & Y_2'^{(6)} & Y_3'^{(6)} \end{pmatrix} \right]_{RL}, \quad (20)$$

where assignments of representations and weights for MSSM fields are given in Table 2.

	Q	(d^c, s^c, b^c)	(u^c, c^c, t^c)	$H_{u,d}$	$\mathbf{Y}_3^{(2)}$	$\mathbf{Y}_3^{(6)}, \mathbf{Y}_{3'}^{(6)}$
$SU(2)$	2	1	1	2	1	1
A_4	3	(1, 1'', 1')	(1, 1'', 1')	1	3	3, 3'
$-k_I$	-2	(0, 0, 0)	(-4, -4, -4)	0	$k = 2$	$k = 6$

Table 2: Assignments of representations and weights $-k_I$ for MSSM fields and modular forms of weight 2 and 6 in model-I.

Model-II : down-type quark mass matrix with $\mathbf{Y}_3^{(6)}$ and $\mathbf{Y}_{3'}^{(6)}$ and up-type one with $\mathbf{Y}_3^{(2)}$

$$M_d = v_d \begin{pmatrix} \alpha_d & 0 & 0 \\ 0 & \beta_d & 0 \\ 0 & 0 & \gamma_d \end{pmatrix} \left[\begin{pmatrix} Y_2^{(6)} & Y_3^{(6)} & Y_1^{(6)} \\ Y_3^{(6)} & Y_1^{(6)} & Y_2^{(6)} \\ Y_1^{(6)} & Y_2^{(6)} & Y_3^{(6)} \end{pmatrix} + g_d \begin{pmatrix} Y_2'^{(6)} & Y_3'^{(6)} & Y_1'^{(6)} \\ Y_3'^{(6)} & Y_1'^{(6)} & Y_2'^{(6)} \\ Y_1'^{(6)} & Y_2'^{(6)} & Y_3'^{(6)} \end{pmatrix} \right]_{RL},$$

$$M_u = v_u \begin{pmatrix} \alpha_u & 0 & 0 \\ 0 & \beta_u & 0 \\ 0 & 0 & \gamma_u \end{pmatrix} \begin{pmatrix} Y_2 & Y_3 & Y_1 \\ Y_3 & Y_1 & Y_2 \\ Y_1 & Y_2 & Y_3 \end{pmatrix}_{RL}, \quad (21)$$

where assignments of representations and weights for MSSM fields are given in Table 3.

	Q	(d^c, s^c, b^c)	(u^c, c^c, t^c)	$H_{u,d}$	$\mathbf{Y}_3^{(2)}$	$\mathbf{Y}_3^{(6)}, \mathbf{Y}_{3'}^{(6)}$
$SU(2)$	2	1	1	2	1	1
A_4	3	(1, 1'', 1')	(1, 1'', 1')	1	3	3, 3'
$-k_I$	-2	(-4, -4, -4)	(0, 0, 0)	0	$k = 2$	$k = 6$

Table 3: Assignments of representations and weights $-k_I$ for MSSM fields and modular forms of weight 2 and 6 in model-II.

Model-III : both down-type quark mass matrix and up-type one with $\mathbf{Y}_3^{(6)}$ and $\mathbf{Y}_{3'}^{(6)}$

$$M_d = v_d \begin{pmatrix} \alpha_d & 0 & 0 \\ 0 & \beta_d & 0 \\ 0 & 0 & \gamma_d \end{pmatrix} \left[\begin{pmatrix} Y_2^{(6)} & Y_3^{(6)} & Y_1^{(6)} \\ Y_3^{(6)} & Y_1^{(6)} & Y_2^{(6)} \\ Y_1^{(6)} & Y_2^{(6)} & Y_3^{(6)} \end{pmatrix} + g_d \begin{pmatrix} Y_2'^{(6)} & Y_3'^{(6)} & Y_1'^{(6)} \\ Y_3'^{(6)} & Y_1'^{(6)} & Y_2'^{(6)} \\ Y_1'^{(6)} & Y_2'^{(6)} & Y_3'^{(6)} \end{pmatrix} \right]_{RL},$$

$$M_u = v_u \begin{pmatrix} \alpha_u & 0 & 0 \\ 0 & \beta_u & 0 \\ 0 & 0 & \gamma_u \end{pmatrix} \left[\begin{pmatrix} Y_2^{(6)} & Y_3^{(6)} & Y_1^{(6)} \\ Y_3^{(6)} & Y_1^{(6)} & Y_2^{(6)} \\ Y_1^{(6)} & Y_2^{(6)} & Y_3^{(6)} \end{pmatrix} + g_u \begin{pmatrix} Y_2'^{(6)} & Y_3'^{(6)} & Y_1'^{(6)} \\ Y_3'^{(6)} & Y_1'^{(6)} & Y_2'^{(6)} \\ Y_1'^{(6)} & Y_2'^{(6)} & Y_3'^{(6)} \end{pmatrix} \right]_{RL}, \quad (22)$$

where assignments of representations and weights for MSSM fields are given in Table 4. We discuss numerical results of these three models in the next section.

	Q	(d^c, s^c, b^c)	(u^c, c^c, t^c)	$H_{u,d}$	$\mathbf{Y}_3^{(6)}, \mathbf{Y}_{3'}^{(6)}$
$SU(2)$	2	1	1	2	1
A_4	3	$(\mathbf{1}, \mathbf{1}'', \mathbf{1}')$	$(\mathbf{1}, \mathbf{1}'', \mathbf{1}')$	1	3 , 3'
$-k_I$	-2	$(-4, -4, -4)$	$(-4, -4, -4)$	0	$k = 6$

Table 4: Assignments of representations and weights $-k_I$ for MSSM fields and modular forms of weight 6 in model-III.

4 Numerical results of CKM mixing

In order to obtain the left-handed flavor mixing, we calculate $M_d^\dagger M_d$ and $M_u^\dagger M_u$ for model-I, model-II and model-III, respectively. At first, we take a random point of τ and g_q which are scanned in the complex plane by generating random numbers. The scanned ranges of $\text{Im}[\tau]$ is $[0.5, 10]$, in which the lower-cut 0.5 comes from the accuracy of calculating modular forms, and the upper-cut 10 is enough large for estimating Y_i in practice. On the other hand, $\text{Re}[\tau]$ is scanned in the fundamental region $[-3/2, 3/2]$ of A_4 in Eq.(10). We also scan in $|g_u| \in [0, 2000]$ and $|g_d| \in [0, 2000]$ while these phases are scanned in $[-\pi, \pi]$. Then, parameters $\alpha_q, \beta_q, \gamma_q$ ($q = u, d$) are determined by computing forms $C_i^q (i = 1-3)$ in Appendix B after inputting six quark masses (see Appendix B).

Finally, we calculate three CKM mixing angles in terms of the model parameters τ, g_q . We keep the parameter sets, in which the value of each observable is reproduced within its respective experimentally allowed 3σ interval. We continue this procedure to obtain enough points for plotting allowed region.

We input quark masses in order to constrain model parameters. Since the modulus τ obtains the expectation value by the breaking of the modular invariance at the high mass scale, the quark masses are put at the GUT scale. The observed masses and CKM parameters run to the GUT scale by the renormalization group equations (RGEs). In our work, we adopt numerical values of Yukawa couplings of quarks at the GUT scale 2×10^{16} GeV with $\tan \beta = 5$ in the framework of the minimal SUSY breaking scenarios [57, 58]:

$$y_d = (4.81 \pm 1.06) \times 10^{-6}, \quad y_s = (9.52 \pm 1.03) \times 10^{-5}, \quad y_b = (6.95 \pm 0.175) \times 10^{-3},$$

$$y_u = (2.92 \pm 1.81) \times 10^{-6}, \quad y_c = (1.43 \pm 0.100) \times 10^{-3}, \quad y_t = 0.534 \pm 0.0341, \quad (23)$$

which give quark masses as $m_q = y_q v_H$ with $v_H = 174$ GeV. We also use the following CKM mixing angles to focus on parameter regions consistent with the experimental data at the GUT scale 2×10^{16} GeV, where $\tan \beta = 5$ is taken [57, 58]:

$$\theta_{12} = 13.027^\circ \pm 0.0814^\circ, \quad \theta_{23} = 2.054^\circ \pm 0.384^\circ, \quad \theta_{13} = 0.1802^\circ \pm 0.0281^\circ. \quad (24)$$

Here θ_{ij} is given in the PDG notation of the CKM matrix V_{CKM} [59]. The error intervals in Eqs.(23) and (24) represent 1σ interval. In our numerical calculation, we take 2σ interval for quark masses.

In the model-I, we have four real parameters, that is, free complex parameters τ and g_u after inputting six quark masses. By constraining these parameters by three CKM mixing angles in Eq.(24) with 3σ interval, we can predict the CP violating phase δ_{CP} , which is given in the PDG notation [59]. We show the predicted δ_{CP} versus the CKM element $|V_{ub}|$ in Fig.1, in which δ_{CP} should be compared with the observed one at the GUT scale 2×10^{16} GeV with $\tan \beta = 5$ [57, 58]:

$$\delta_{CP} = 69.21^\circ \pm 6.19^\circ. \quad (25)$$

The predicted region is symmetric about the horizontal line of 180° . Some points are consistent with the experimental value of δ_{CP} with 3σ interval. They are rather lower value 50° – 55° . However, we should take into account that the input parameters of Yukawa couplings in Eq.(23) are specific ones at $\tan \beta = 5$. We have checked that the predicted δ_{CP} increases up to 10% according to decrease of $\tan \beta$ towards 1. Numerical results of Yukawa couplings at the GUT scale also depend on the SUSY breaking scenario and its scale. Moreover, we have found that the predicted range of δ_{CP} is enlarged with $\pm 10^\circ$ if 3σ error-bar is taken for the input masses of Eq.(23) while quark masses with 2σ interval are input in Fig.1. Therefore, the predicted δ_{CP} could be close to the central value of Eq.(25) if the input quark masses are taken relevantly. In conclusion, our predicted CP violating phase of model-I is completely consistent with the observed one.

We also show the allowed region of CKM elements $|V_{cb}|$ and $|V_{ub}|$ in Fig.2, where green (blue) points denote allowed ones with (without) constraint of observed δ_{CP} . The magnitude of V_{cb} is predicted to be larger than the central value while calculated $|V_{ub}|$ is close to the lower bound of

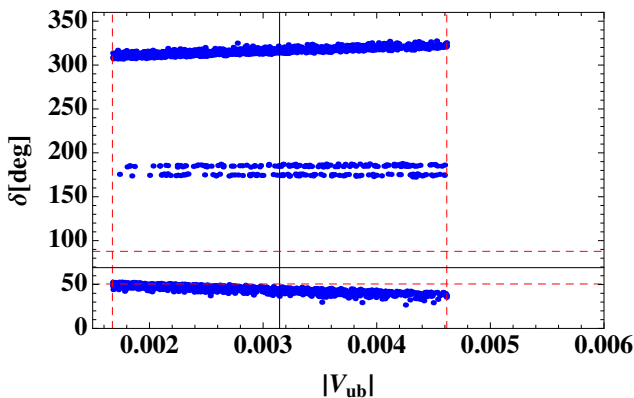


Figure 1: Predicted δ_{CP} versus $|V_{ub}|$, where black lines denote observed central values of $|V_{ub}|$ and δ_{CP} , and red dashed-lines denote their upper-bounds and lower-bounds of 3σ interval in model-I.

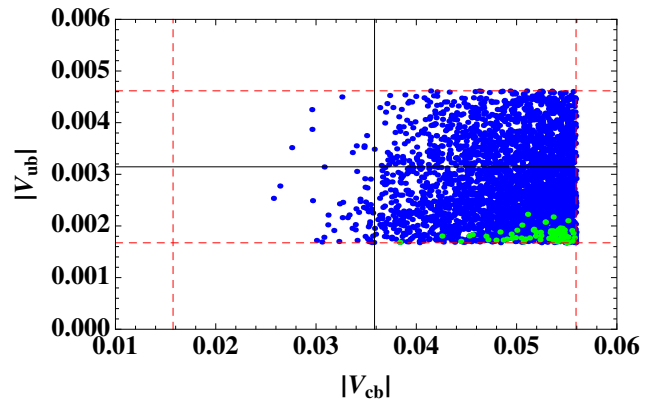


Figure 2: Allowed region on $|V_{cb}|$ – $|V_{ub}|$ plane in model-I. Notation of black and red lines are same ones in Fig.1. Blue (green) points denote allowed ones without (with) constraint of observed δ_{CP} .

the experimental data under the constraint of the observed δ_{CP} . Those predictions are also relaxed if the input quark masses are taken relevantly.

In the model-II, we have also four real parameters, that is, free complex parameters τ and g_d after inputting six quark masses. However, there is no allowed points consistent with three CKM mixing angles. The Cabibbo mixing angle and $|V_{cb}|$ are easily reproduced by choosing relevant values for our parameters, but $|V_{ub}|$ is unavoidably around the magnitude of V_{cb} .

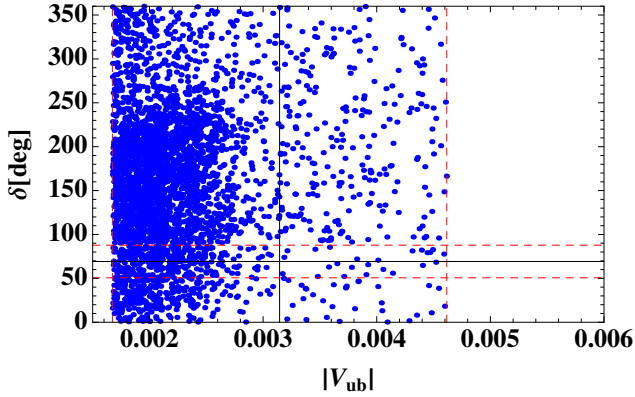


Figure 3: Predicted δ_{CP} versus $|V_{ub}|$, where black lines denote observed central values of $|V_{ub}|$ and δ_{CP} , and red dashed-lines denote their upper-bounds and lower-bounds of 3σ interval in model-III.

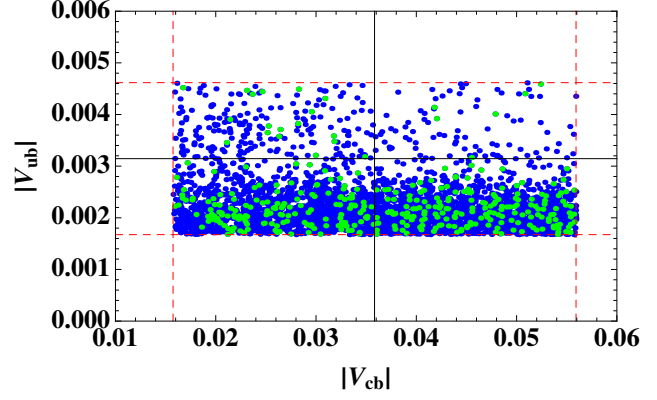


Figure 4: Allowed region on $|V_{cb}|$ - $|V_{ub}|$ plane in model-III. Notations of black and red lines are same ones in Fig.3. Blue (green) points denote allowed ones without (with) constraint of observed δ_{CP} .

Finally, we present the numerical result of model-III, where we have three complex parameters, τ , g_d and g_u after inputting six quark masses. That is, there are two additional real parameters in contrast with model-I and model-II. These additional parameters are available to reproduce the observed CKM elements. We show δ_{CP} versus $|V_{ub}|$ by constraining parameters with three CKM mixing angles of Eq.(24) in Fig.3. The predicted δ_{CP} covers $0-2\pi$ and symmetric about the horizontal line of 180° . Thus, model-III allows any value for δ_{CP} . Model parameters are restricted by imposing the observed CP violating phase as seen in Table 5.

We also show the allowed region of $|V_{cb}|$ and $|V_{ub}|$ in Fig.4, where green (blue) points denote

	Model I	Model III
$\text{Re}[\tau]$	$\pm(0.95-1.05)$ $-0.05-0.05$	$\pm(0.11-1.50)$
$\text{Im}[\tau]$	$0.95-1.05$	$1.20-1.59$
$\text{Re}[g_u]$	$-(0.14-0.15)$	$\pm(0.001-0.08)$
$\text{Im}[g_u]$	$0.20-0.21$	$\pm(0.001-0.14)$
$\text{Re}[g_d]$	—	$\pm(162-1459)$
$\text{Im}[g_d]$	—	$\pm(0.1-996)$

Table 5: Parameter ranges consistent with the observed CKM mixing angles and CP violating phase δ_{CP} for model-I and model-III, respectively.

allowed ones with (without) constraint of observed δ_{CP} . The magnitude of V_{ub} is preferred to be smaller than the central value while calculated $|V_{cb}|$ covers all range of the experimental data.

In Table 5, we summarize parameter ranges consistent with observed CKM mixing angles and the CP violating phase for both model-I and model-III. It is noticed that the imaginary part of g_q is inevitable to reproduce the observed δ_{CP} in addition to $\text{Re}[\tau]$, which provides imaginary parts in q , $q^{1/3}$ and $q^{2/3}$ as seen in Eq.(11).

In Table 6, we show typical parameter sets and calculated CKM parameters in model-I and model-III, respectively. Ratios of α_q/γ_q and β_q/γ_q ($q = u, d$) in Table 6 correspond to the observed quark mass hierarchy.

	Model-I	Model-III
τ	$0.038 + 0.999 i$	$-1.130 + 1.552 i$
g_u	$-0.141 - 0.201 i$	$-0.026 + 0.077 i$
g_d	—	$1334 + 9.7 i$
α_u/γ_u	1.637×10^2	8.221×10^4
β_u/γ_u	5.734×10^3	3.372×10^6
α_d/γ_d	4.402×10^0	1.744
β_d/γ_d	2.716×10^2	3.500×10^3
$ V_{us} $	0.2237	0.2282
$ V_{cb} $	0.0472	0.0357
$ V_{ub} $	0.0017	0.0019
δ_{CP}	51.1°	79.0°

Table 6: Numerical values of parameters and output of CKM parameters at the sample points for model-I and model-III, respectively.

We also present the mixing matrices of down-type quarks and up-type quarks for two samples in order to investigate the flavor structure of each quark mass matrix. For the sample of model-I in Table 6, we obtain

$$\begin{aligned}
V_d &\approx \begin{pmatrix} -0.578 & -0.578 & -0.5756 \\ 0.785 + 0.061i & -0.211 - 0.026i & -0.577 - 0.036i \\ -0.212 + 0.016i & 0.782 - 0.095i & -0.573 + 0.079i \end{pmatrix}, \\
V_u &\approx \begin{pmatrix} -0.499 & -0.670 & -0.549 \\ 0.786 - 0.143i & -0.114 + 0.131i & -0.576 - 0.030i \\ -0.247 + 0.228i & 0.670 - 0.269i & -0.593 + 0.120i \end{pmatrix},
\end{aligned} \tag{26}$$

where $V_{\text{CKM}} = V_u^\dagger V_d$. It is noticed that magnitudes of mixing elements are of same order in both rotation matrices. The observed CKM matrix is realized by the relevant cancellation between the down-type and up-type quark sectors. We have checked that the quark mixing matrices are likely in Eq.(26) for all parameter sets of model-I. The hierarchical structure can be realized on the different basis of generators S and T from the one in Eq.(9). This work will be presented elsewhere.

For the sample of model-III in Table 6, we have

$$\begin{aligned} V_d &\approx \begin{pmatrix} -0.0184 & -0.9737 & 0.2271 \\ -0.662 + 0.745i & -0.0275i & -0.0563 - 0.0574i \\ -0.0644 - 0.0522i & -0.161 + 0.158i & -0.697 + 0.675i \end{pmatrix}, \\ V_u &\approx \begin{pmatrix} -0.2175 & 0.9514 & 0.2179 \\ -0.580 - 0.785i & -0.119 - 0.168i & -0.0571 - 0.0496i \\ 0.0284 - 0.0103i & 0.141 - 0.180i & -0.586 + 0.777i \end{pmatrix}. \end{aligned} \quad (27)$$

After exchanging rows between 1st and 2nd ones, those are typical hierarchical mixing matrices. These exchanges correspond to $(t_L, c_L, u_L) \rightarrow (t_L, u_L, c_L)$ and $(b_L, s_L, d_L) \rightarrow (b_L, d_L, s_L)$ for the assignment of the A_4 triplet. It is noted that the quark mass matrices are also hierarchical for other parameter sets of model-III.

In conclusion, our quark mass matrices with the A_4 modular symmetry (model-I and model-III) can successfully reproduce the CKM mixing matrix completely with observed quark masses. This successful result encourages us to investigate the lepton sector in the same framework. We discuss the lepton mass matrices with the A_4 modular symmetry in the next section.

5 Lepton mass matrix in the A_4 modular invariance

5.1 Lepton mass matrix

The modular A_4 invariance also gives the lepton mass matrix in terms of the modulus τ which is common both quarks and leptons if flavors of quarks and leptons are originated from a same two-dimensional compact space. The A_4 representation and weight are assigned for lepton fields relevantly as seen in Table 7, where the left-handed lepton doublets compose a A_4 triplet and the right-handed charged leptons are A_4 singlets. Weights of leptons are assigned like as the quark ones in Table 7.

	L	(e^c, μ^c, τ^c)	H_u	H_d	$\mathbf{Y}_r^{(2)}, \mathbf{Y}_r^{(4)}$
$SU(2)$	2	1	2	2	1
A_4	3	(1, 1'', 1')	1	1	3, {3, 1, 1'}
$-k_I$	-2	(0, 0, 0) or (-4, -4, -4)	0	0	2, 4

Table 7: Assignments of representations and weights $-k_I$ for MSSM fields and modular forms of weight 2 and 4.

Assign the left-handed charged leptons a A_4 triplet $L = (e_L, \mu_L, \tau_L)$ in order of the charged lepton mass hierarchy. The charged lepton mass matrix $M_E^{(k)}$ is given in terms of modular forms of weight 6, $\mathbf{Y}_3^{(6)}$ or of weight 2, $\mathbf{Y}_3^{(2)}$ by assigning weight -4 or 0 to right-handed charged leptons, respectively. It is presented as:

$$M_E^{(6)} = v_d \begin{pmatrix} \alpha_e & 0 & 0 \\ 0 & \beta_e & 0 \\ 0 & 0 & \gamma_e \end{pmatrix} \left[\begin{pmatrix} Y_1^{(6)} & Y_3^{(6)} & Y_2^{(6)} \\ Y_2^{(6)} & Y_1^{(6)} & Y_3^{(6)} \\ Y_3^{(6)} & Y_2^{(6)} & Y_1^{(6)} \end{pmatrix} + g_e \begin{pmatrix} Y_1'^{(6)} & Y_3'^{(6)} & Y_2'^{(6)} \\ Y_2'^{(6)} & Y_1'^{(6)} & Y_3'^{(6)} \\ Y_3'^{(6)} & Y_2'^{(6)} & Y_1'^{(6)} \end{pmatrix} \right]_{RL}, \quad (28)$$

$$M_E^{(2)} = v_d \begin{pmatrix} \alpha_e & 0 & 0 \\ 0 & \beta_e & 0 \\ 0 & 0 & \gamma_e \end{pmatrix} \begin{pmatrix} Y_1 & Y_3 & Y_2 \\ Y_2 & Y_1 & Y_3 \\ Y_3 & Y_2 & Y_1 \end{pmatrix}_{RL}, \quad (29)$$

where we take a common g_e in Eq.(28) for three families likely in the quark mass matrix. Coefficients α_e , β_e and γ_e are real parameters while g_e is complex one.

Suppose neutrinos to be Majorana particles. By using the Weinberg operator, the superpotential of the neutrino mass term, w_ν is given as:

$$w_\nu = -\frac{1}{\Lambda} (H_u H_u L L \mathbf{Y}_r^{(k)})_1, \quad (30)$$

where Λ is a relevant cut off scale. Since the left-handed lepton doublet has weight -2 , the superpotential is given in terms of modular forms of weight 4, $\mathbf{Y}_3^{(4)}$, $\mathbf{Y}_1^{(4)}$ and $\mathbf{Y}_{1'}^{(4)}$.

By putting the vacuum expectation value of H_u (v_u) and taking $L = (\nu_e, \nu_\mu, \nu_\tau)$ for neutrinos, we have

$$\begin{aligned} w_\nu &= \frac{v_u^2}{\Lambda} \left[\begin{pmatrix} 2\nu_e\nu_e - \nu_\mu\nu_\tau - \nu_\tau\nu_\mu \\ 2\nu_\tau\nu_\tau - \nu_e\nu_\mu - \nu_\mu\nu_\tau \\ 2\nu_\mu\nu_\mu - \nu_\tau\nu_e - \nu_e\nu_\tau \end{pmatrix} \otimes \mathbf{Y}_3^{(4)} \right. \\ &\quad \left. + (\nu_e\nu_e + \nu_\mu\nu_\tau + \nu_\tau\nu_\mu) \otimes g_{\nu 1} \mathbf{Y}_1^{(4)} + (\nu_e\nu_\tau + \nu_\mu\nu_\mu + \nu_\tau\nu_e) \otimes g_{\nu 2} \mathbf{Y}_{1'}^{(4)} \right] \\ &= \frac{v_u^2}{\Lambda} \left[(2\nu_e\nu_e - \nu_\mu\nu_\tau - \nu_\tau\nu_\mu) Y_1^{(4)} + (2\nu_\tau\nu_\tau - \nu_e\nu_\mu - \nu_\mu\nu_e) Y_3^{(4)} + (2\nu_\mu\nu_\mu - \nu_\tau\nu_e - \nu_e\nu_\tau) Y_2^{(4)} \right. \\ &\quad \left. + (\nu_e\nu_e + \nu_\mu\nu_\tau + \nu_\tau\nu_\mu) g_{\nu 1} \mathbf{Y}_1^{(4)} + (\nu_e\nu_\tau + \nu_\mu\nu_\mu + \nu_\tau\nu_e) g_{\nu 2} \mathbf{Y}_{1'}^{(4)} \right], \quad (31) \end{aligned}$$

where $\mathbf{Y}_3^{(4)}$, $\mathbf{Y}_1^{(4)}$ and $\mathbf{Y}_{1'}^{(4)}$ are given in Eq.(13), and $g_{\nu 1}$, $g_{\nu 2}$ are complex parameters. The neutrino mass matrix is written as follows:

$$M_\nu = \frac{v_u^2}{\Lambda} \left[\begin{pmatrix} 2Y_1^{(4)} & -Y_3^{(4)} & -Y_2^{(4)} \\ -Y_3^{(4)} & 2Y_2^{(4)} & -Y_1^{(4)} \\ -Y_2^{(4)} & -Y_1^{(4)} & 2Y_3^{(4)} \end{pmatrix} + g_{\nu 1} \mathbf{Y}_1^{(4)} \begin{pmatrix} 1 & 0 & 0 \\ 0 & 0 & 1 \\ 0 & 1 & 0 \end{pmatrix} + g_{\nu 2} \mathbf{Y}_{1'}^{(4)} \begin{pmatrix} 0 & 0 & 1 \\ 0 & 1 & 0 \\ 1 & 0 & 0 \end{pmatrix} \right]_{LL}. \quad (32)$$

Model parameters are α_e , β_e , γ_e , (g_e) , $g_{\nu 1}$ and $g_{\nu 2}$. Parameters α_e , β_e and γ_e are adjusted by the observed charged lepton masses as given in Appendix B. Therefore, the lepton mixing angles, the Dirac phase and Majorana phases are given by $g_{\nu 1}$, (g_e) and $g_{\nu 2}$ in addition to the value of τ . Since τ is restricted in the narrow range for the model-I of the quark sector as seen in Table 5, we expect to get predictions in the lepton mixing.

5.2 Numerical results of leptons

We input charged lepton masses in order to constrain the model parameters. We take Yukawa couplings of charged leptons at the GUT scale 2×10^{16} GeV, where $\tan \beta = 5$ is taken as well as quark Yukawa couplings [57, 58]:

$$y_e = (1.97 \pm 0.024) \times 10^{-6}, \quad y_\mu = (4.16 \pm 0.050) \times 10^{-4}, \quad y_\tau = (7.07 \pm 0.073) \times 10^{-3}, \quad (33)$$

where lepton masses are given by $m_\ell = y_\ell v_H$ with $v_H = 174$ GeV. We also use the following lepton mixing angles and neutrino mass parameters, which are given by NuFit 4.0 in Table 8 [60]. Since there are two possible spectrum of neutrinos masses m_i , which are the normal hierarchy (NH), $m_3 > m_2 > m_1$, and the inverted hierarchy (IH), $m_2 > m_1 > m_3$, we investigate both cases.

observable	3σ range for NH	3σ range for IH
Δm_{atm}^2	$(2.431\text{--}2.622) \times 10^{-3} \text{eV}^2$	$-(2.413\text{--}2.606) \times 10^{-3} \text{eV}^2$
Δm_{sol}^2	$(6.79\text{--}8.01) \times 10^{-5} \text{eV}^2$	$(6.79\text{--}8.01) \times 10^{-5} \text{eV}^2$
$\sin^2 \theta_{23}$	0.428–0.624	0.433–0.623
$\sin^2 \theta_{12}$	0.275–0.350	0.275–0.350
$\sin^2 \theta_{13}$	0.02044–0.02437	0.02067–0.02461

Table 8: The 3σ ranges of neutrino parameters from NuFIT 4.0 for NH and IH [60].

Neutrino masses and the PMNS matrix U_{PMNS} [61, 62] are obtained by diagonalizing $M_E^{(k)\dagger} M_E^{(k)}$ and $M_\nu^* M_\nu$. We also investigate the sum of three neutrino masses $\sum m_i$ in our model since it is constrained by the recent cosmological data, 120meV [63, 64]. The effective mass for the $0\nu\beta\beta$ decay is given as follows:

$$\langle m_{ee} \rangle = \left| m_1 c_{12}^2 c_{13}^2 + m_2 s_{12}^2 c_{13}^2 e^{i\alpha_{21}} + m_3 s_{13}^2 e^{i(\alpha_{31} - 2\delta_{CP}^\ell)} \right|, \quad (34)$$

where δ_{CP}^ℓ is the Dirac phase of leptons, and α_{21} , α_{31} are Majorana phases as seen in Appendix C.

Let us discuss numerical result for the case of the charged lepton mass matrix $M_E^{(6)}$ of Eq.(28) in NH of neutrino masses. At first, we show the allowed region $\text{Re}[\tau]$ – $\text{Im}[\tau]$ plane in Fig.5. Observed three mixing angles of leptons are reproduced at green, blue and red points while observed CKM elements are obtained at brown points for model-I of quarks and magenta points for model-III of quarks, respectively. Especially, both observed quark CKM elements and lepton mixing angles are reproduced at red points. It is noted that green and red points almost overlap. The T symmetry of Eq.(2), that is the $\tau \rightarrow \tau + 1$ shift symmetry, is clearly seen in Fig.5. It is also noticed that blue points and green ones are related with the S symmetry of Eq.(2), that is $\tau \rightarrow -1/\tau$.

Remarkably, there are common regions around $\text{Im}[\tau] = 1$ and $\text{Re}[\tau] = 0, \pm 1$ of quarks and leptons only for model-I. It is emphasized that $\tau = i$ is a fixed point in the fundamental region of $\text{SL}(2, Z)$, which indicates the residual symmetry Z_2 . Indeed, we reproduce both CKM parameters ($|V_{us}|$, $|V_{cb}|$, $|V_{ub}|$, δ_{CP}), and PMNS mixing angles (θ_{12} , θ_{23} , θ_{13}), which are consistent with experimental data at the common τ . There is no common τ of quarks and leptons for model-III of quarks.

We have five complex parameters τ , g_u , g_e , $g_{\nu 1}$ and $g_{\nu 2}$ after inputting quarks and charged lepton masses in the framework of model-I of quarks and the charged lepton mass matrix $M_E^{(6)}$. These five complex parameters are constrained by eight observed quantities; the four observed CKM elements, three mixing angles of leptons and observed mass ratio $\Delta m_{\text{sol}}^2/\Delta m_{\text{atm}}^2$, namely, τ is constrained considerably by the experimental data. Therefore, we can predict the CP violating phase δ_{CP}^ℓ , Majorana phases α_{21} , α_{31} , the effective mass $\langle m_{ee} \rangle$ for the $0\nu\beta\beta$ decay and the sum of neutrino masses.

We show the predicted δ_{CP}^ℓ versus $\sin^2 \theta_{23}$ in Fig.6, where colors (blue, green and red) of points correspond to points of τ in Fig.5. Red points denote common values of τ in both quark and lepton mass matrices. At the red point region, we predict rather broad range, $\delta_{CP}^\ell = 20^\circ\text{--}150^\circ$ and $210^\circ\text{--}340^\circ$, which is consistent with the recent observations [44,45]. On the other hand, $\sin^2 \theta_{23}$ is allowed in $0.428\text{--}0.624$, which is observed range with 3σ . The precise determination of $\sin^2 \theta_{23}$ help us to predict δ_{CP}^ℓ .

We also present the prediction of Majorana phases on the $\alpha_{21}\text{--}\alpha_{31}$ plane in Fig.7. At the red point region, α_{21} is restricted in $60^\circ\text{--}80^\circ$, $130^\circ\text{--}230^\circ$, $280^\circ\text{--}300^\circ$ and around 0° while α_{31} is allowed in $(0, 2\pi)$. The predicted region is broad without inputs of CKM parameters of the quark sector.

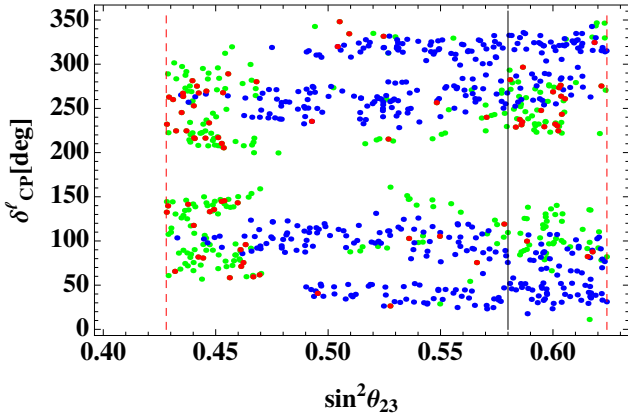


Figure 6: Predicted δ_{CP}^ℓ versus $\sin^2 \theta_{23}$, where black line denotes observed best-fit value of $\sin^2 \theta_{23}$, and red dashed-lines denote its upper(lower)-bound of 3σ interval for $M_E^{(6)}$ in the case of NH. Colors of points correspond to points of τ in Fig.5. At red points, the common τ is realized in leptons and quarks of model-I.

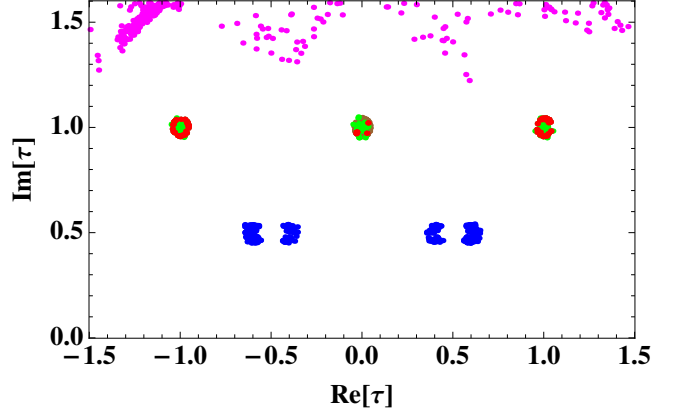


Figure 5: The allowed regions of τ for $M_E^{(6)}$. Observed lepton mixing angles are reproduced at green, blue and red points while observed CKM are reproduced at brown and magenta points in model-I and III, respectively. Both CKM and PMNS are reproduced at red points, which almost overlap with green ones.

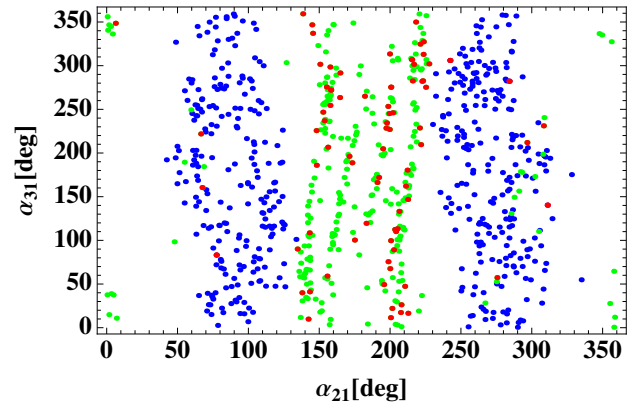


Figure 7: Predicted region of Majorana phases in the $\alpha_{21}\text{--}\alpha_{31}$ plane, for $M_E^{(6)}$ in the case of NH. Colors of points correspond to points of τ in Fig.5. At red points, the common τ is realized in leptons and quarks of model-I.

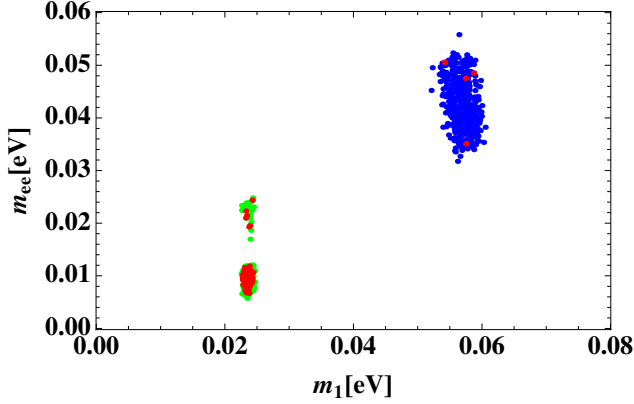


Figure 8: Predicted effective mass $\langle m_{ee} \rangle$ of the $0\nu\beta\beta$ decay versus m_1 for $M_E^{(6)}$ in the case of NH. Red points have common τ in leptons and quarks of model-I.

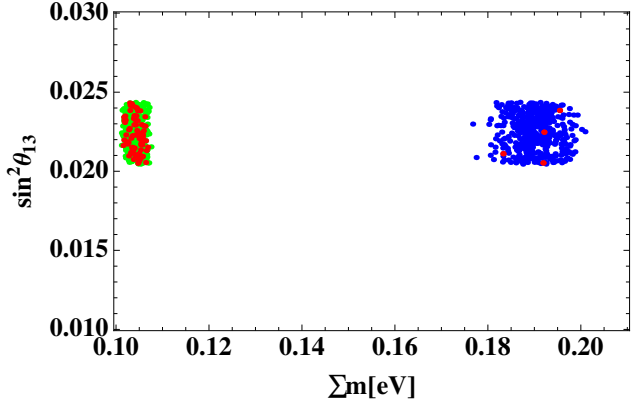


Figure 9: Sum of masses and $\sin^2 \theta_{13}$ for $M_E^{(6)}$ in the case of NH, where $\sin^2 \theta_{13}$ is cut at the observed 3σ interval. Red points have common τ in leptons and quarks of model-I.

By using these Majorana phases, we can predict the effective mass $\langle m_{ee} \rangle$ for the $0\nu\beta\beta$ decay versus the lightest mass m_1 as seen in Fig.8. At the red point region, we predict $\langle m_{ee} \rangle = 5\text{--}12\text{meV}$ and $19\text{--}24\text{meV}$ while we have $m_1 = 23\text{--}25\text{meV}$. The predicted m_{ee} larger than 30meV (blue points and red ones in Fig.8) is excluded by the sum of neutrino masses in Fig. 9.

We also show $\sin^2 \theta_{13}$ versus the sum of neutrino masses $\sum m_i$ in Fig.9. At the red point region, we obtain $\sum m_i \simeq 102\text{--}107\text{meV}$, which is consistent with the cosmological upper-bound of the sum of neutrino masses 120meV . The $\sin^2 \theta_{13}$ is consistent with observed one $0.02044\text{--}0.02437$ in Table 8. The update of the cosmological upper-bound of the sum of neutrino masses provides a severe test for our model. The figure of the calculated $\sin^2 \theta_{12}$ is omitted in this paper. At red points of τ , it is distributed in the overall range of the experimental data with 3σ error-bar. Thus, our charged lepton mass matrix $M_E^{(6)}$ could be consistent with quark sector with the common τ .

Next, we discuss numerical result for the case of the charged lepton mass matrix $M_E^{(2)}$ of Eq.(29) for NH of neutrino masses with keeping the neutrino mass matrix in Eq.(32). We show the allowed region on the $\text{Re}[\tau]\text{--}\text{Im}[\tau]$ plane, where PMNS mixing angles θ_{12} , θ_{23} and θ_{13} are consistent with experimental data for NH of neutrino masses, in Fig.10. Observed three mixing angles of leptons are reproduced at green and blue points while observed CKM elements are obtained at brown points for model-I of quarks

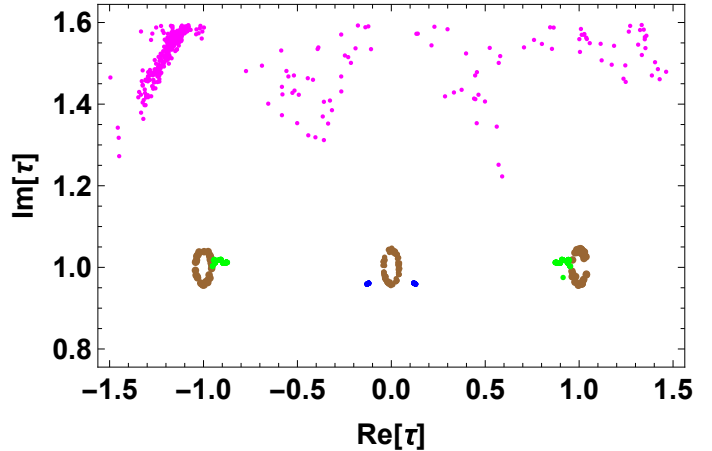


Figure 10: Allowed region on $\text{Re}[\tau]\text{--}\text{Im}[\tau]$ plane for $M_E^{(2)}$ in the case of NH. Observed mixing angles of leptons are reproduced at green, blue while CKM elements are reproduced at brown and magenta points in model-I and model-III, respectively. There is no overlapping region between CKM and lepton mixing angles.

and blue points while observed CKM elements are obtained at brown points for model-I of quarks

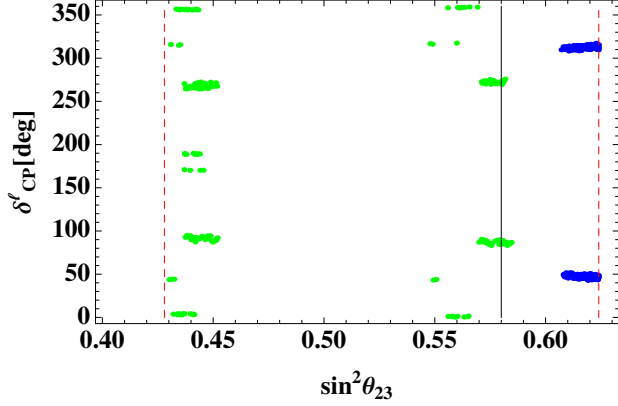


Figure 11: Predicted δ_{CP}^ℓ versus $\sin^2 \theta_{23}$, where black line denotes observed best-fit value of $\sin^2 \theta_{23}$, and red dashed-lines denote its upper(lower)-bound of 3σ interval for $M_E^{(2)}$ in the case of NH. Colors of points correspond to points of τ in Fig.10.

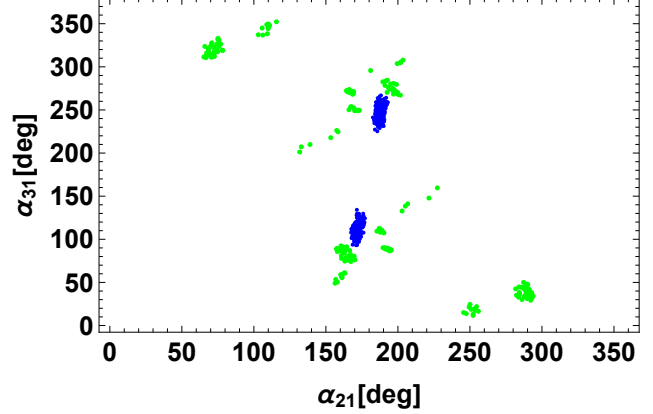


Figure 12: Predicted region of Majorana phases in the α_{21} - α_{31} plane, for $M_E^{(2)}$ in the case of NH. Colors of points correspond to points of τ in Fig.10.

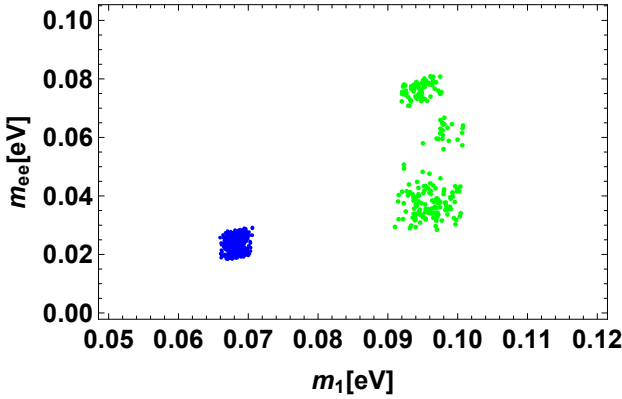


Figure 13: Predicted effective mass $\langle m_{ee} \rangle$ of the $0\nu\beta\beta$ decay versus m_1 for $M_E^{(2)}$ in the case of NH.

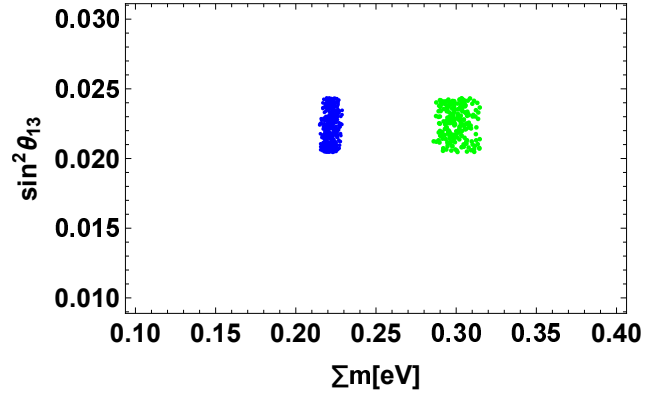


Figure 14: Sum of masses and $\sin^2 \theta_{13}$ for $M_E^{(2)}$ in the case of NH, where $\sin^2 \theta_{13}$ is cut at the observed 3σ interval.

and magenta points for model-III of quarks, respectively ³. It is noticed that there are no common regions of τ of quarks and leptons for both model-I and III although green points are very close to brown ones.

We show four figures, which corresponding to Figs.6, 7, 8 and 9 in the case of $M_E^{(6)}$, although there is no common region of τ of quarks and leptons. The predicted δ_{CP}^ℓ versus $\sin^2 \theta_{23}$ is presented in Fig.11, where colors of points correspond to points of τ in Fig.10. The predicted region of δ_{CP}^ℓ and $\sin^2 \theta_{23}$ are reduced compared with the case of $M_E^{(6)}$.

We also present the prediction of Majorana phases on the α_{21} - α_{31} plane in Fig.12. For α_{21} , (0° - 60°) and (300° - 360°) are completely excluded. On the other hand, α_{31} is allowed in almost

³The shift symmetry $\tau \rightarrow \tau + 1$ of leptons is not seen in Fig.10 since allowed points (green and blue) are not obtained enough.

region of $(0-2\pi)$

By using these Majorana phases, we can predict the effective mass $\langle m_{ee} \rangle$ for the $0\nu\beta\beta$ decay versus the lightest mass m_1 as seen in Fig.13. The predicted $\langle m_{ee} \rangle$ is more than 17meV while m_1 is larger than 66meV. This value leads to the rather large sum of neutrino masses.

We show $\sin^2 \theta_{13}$ versus the sum of neutrino masses $\sum m_i$ in Fig.14. The sum of neutrino masses is larger than 210meV, which is inconsistent with the cosmological upper-bound 120meV. Thus, the charged lepton mass matrix $M_E^{(2)}$ are excluded by the cosmological upper-bound of the sum of neutrino masses, 120meV.

In our numerical calculations, we have not included the RGE effects in the lepton mixing angles and neutrino mass ratio $\Delta m_{\text{sol}}^2 / \Delta m_{\text{atm}}^2$. We suppose that those corrections are very small between the electroweak and GUT scales for NH of neutrino masses. This assumption is justified well in the case of $\tan \beta \leq 5$ unless neutrino masses are almost degenerate [26].

	$M_E^{(6)}$
τ	$-0.0168 + 1.0035 i$
$g_{\nu 1}$	$-0.2805 + 0.2208 i$
$g_{\nu 2}$	$0.7766 + 0.1418 i$
g_e	$-0.2360 + 0.9825 i$
α_e / γ_e	56.48
β_e / γ_e	241.60
$\sin^2 \theta_{12}$	0.304
$\sin^2 \theta_{23}$	0.602
$\sin^2 \theta_{13}$	0.0217
δ_{CP}^ℓ	273°

Table 9: Numerical values of parameters and output of PMNS parameters at the sample point for charged lepton mass matrices $M_E^{(6)}$.

In Table 9, we show a typical parameter set, which gives lepton mixing angles and the Dirac CP phase for the case of the charged lepton mass matrix of $M_E^{(6)}$. It is noticed that ratios of α_e / γ_e and β_e / γ_e in Table 9 due to the observed charged lepton mass hierarchy. It is also remarked that the predicted large CP violating phase δ_{CP} comes from mainly the imaginary parts of $g_{\nu 1}$, $g_{\nu 2}$ and g_e since the real part of the modulus τ is very small.

We also present the mixing matrices of charged leptons and neutrinos for a sample of Table 9. We obtain

$$\begin{aligned}
U_\ell &\approx \begin{pmatrix} -0.618 & -0.462 & -0.635 \\ -0.468 + 0.042i & 0.098 - 0.657i & 0.384 + 0.438i \\ -0.616 + 0.133i & 0.431 + 0.399i & 0.285 - 0.420i \end{pmatrix}, \\
U_\nu &\approx \begin{pmatrix} -0.558 & 0.544 & -0.627 \\ -0.147 - 0.614i & -0.319 - 0.690i & -0.146 - 0.052i \\ -0.503 - 0.193i & 0.352 - 0.053i & 0.752 + 0.126i \end{pmatrix}.
\end{aligned} \tag{35}$$

where $U_{\text{PMNS}} = U_\ell^\dagger U_\nu$. It is noticed that the flavor mixing angles of the charged lepton mass matrix are rather large as well as the neutrino sector in the basis of A_4 generators of S and T of Eq.(9). The hierarchical structure of the charged lepton mass matrix can be realized on the different basis of generators S and T from the one in Eq.(9), which will be presented elsewhere.

Finally, we discuss briefly the case of IH of neutrino masses. For the cases of the charged lepton mass matrix of $M_E^{(6)}$ and $M_E^{(2)}$, we obtain $\langle m_{ee} \rangle = 25\text{--}70\text{meV}$ and $100\text{--}150\text{meV}$, respectively, on the other hand, the sum of neutrino masses to be $160\text{--}330\text{meV}$ and $550\text{--}590\text{meV}$, respectively. Therefore, we conclude that the IH of neutrino masses is excluded for both $M_E^{(6)}$ and $M_E^{(2)}$ due to the cosmological upper bound of neutrino masses.

6 Summary

In this work, we have studied both quarks and leptons in the A_4 modular symmetry towards the unification of quark and lepton flavors. If flavors of quarks and leptons are originated from a same two-dimensional compact space, the quarks and leptons have same flavor symmetry and the same value of the modulus τ . For the quark sector, we have adopted modular forms of weights 2 and 6. We have presented the viable two models for quark mass matrices. The first one (model-I) is that the down-type quark mass matrix is constructed by modular forms of weight 2, but the up-type quark mass matrix is constructed by modular forms of weight 6. Another one (model-III) is that both quark mass matrices are given by modular forms of weight 6. We have also discussed charged lepton mass matrices which are constructed by modular forms of weights 6 and 2, respectively. On the other hands, we have used modular forms of weight 4 for the neutrino mass matrix generated by the Weinberg operator.

For NH of neutrino masses, the charged lepton model with the weight 6 modular forms works well together with the model-I of quarks on the common modulus τ , on the other hand, it does not work with the model-III of quarks. Then, the effective neutrino mass of the $0\nu\beta\beta$ decay is $\langle m_{ee} \rangle = 5\text{--}12\text{meV}$ and $19\text{--}24\text{meV}$. The sum of neutrino masses is $102\text{--}107\text{meV}$. It is remarked that the modulus τ is fixed around $\tau = i$ in the fundamental region of $\text{SL}(2, Z)$, which suggests the residual symmetry Z_2 in the quark and lepton mass matrices. The group theoretical investigation will be presented in the future work. It is also noted that the IH of neutrino masses is excluded by the observed upper bound of the sum of neutrino masses.

Our study provides a new aspect of the unification of the quark and lepton flavors in terms of the modulus τ .

Acknowledgments

This research was supported by an appointment to the JRG Program at the APCTP through the Science and Technology Promotion Fund and Lottery Fund of the Korean Government. This was also supported by the Korean Local Governments - Gyeongsangbuk-do Province and Pohang City (H.O.). H. O. is sincerely grateful for the KIAS member.

Appendix

A Tensor product of A_4 group

We take the generators of A_4 group as follows:

$$S = \frac{1}{3} \begin{pmatrix} -1 & 2 & 2 \\ 2 & -1 & 2 \\ 2 & 2 & -1 \end{pmatrix}, \quad T = \begin{pmatrix} 1 & 0 & 0 \\ 0 & \omega & 0 \\ 0 & 0 & \omega^2 \end{pmatrix}, \quad (36)$$

where $\omega = e^{i\frac{2}{3}\pi}$ for a triplet. In this base, the multiplication rule of the A_4 triplet is

$$\begin{aligned} \begin{pmatrix} a_1 \\ a_2 \\ a_3 \end{pmatrix}_{\mathbf{3}} \otimes \begin{pmatrix} b_1 \\ b_2 \\ b_3 \end{pmatrix}_{\mathbf{3}} &= (a_1 b_1 + a_2 b_3 + a_3 b_2)_{\mathbf{1}} \oplus (a_3 b_3 + a_1 b_2 + a_2 b_1)_{\mathbf{1}'} \\ &\quad \oplus (a_2 b_2 + a_1 b_3 + a_3 b_1)_{\mathbf{1}''} \\ &\quad \oplus \frac{1}{3} \begin{pmatrix} 2a_1 b_1 - a_2 b_3 - a_3 b_2 \\ 2a_3 b_3 - a_1 b_2 - a_2 b_1 \\ 2a_2 b_2 - a_1 b_3 - a_3 b_1 \end{pmatrix}_{\mathbf{3}} \oplus \frac{1}{2} \begin{pmatrix} a_2 b_3 - a_3 b_2 \\ a_1 b_2 - a_2 b_1 \\ a_3 b_1 - a_1 b_3 \end{pmatrix}_{\mathbf{3}}, \\ \mathbf{1} \otimes \mathbf{1} &= \mathbf{1}, \quad \mathbf{1}' \otimes \mathbf{1}' = \mathbf{1}'', \quad \mathbf{1}'' \otimes \mathbf{1}'' = \mathbf{1}', \quad \mathbf{1}' \otimes \mathbf{1}'' = \mathbf{1}. \end{aligned} \quad (37)$$

More details are shown in the review [6, 7].

B α_q/γ_q and β_q/γ_q in terms of quark masses

The coefficients α_q , β_q , and γ_q in Eqs.(17) and (19) are taken to be real positive without loss of generality. These parameters are described in terms of the modulus τ and quark masses. As a representative, we examine the quark mass matrix in Eq. (19) as follows:

$$M_q = v_q \gamma_q \begin{pmatrix} \hat{\alpha}_q & 0 & 0 \\ 0 & \hat{\beta}_q & 0 \\ 0 & 0 & 1 \end{pmatrix} \left[\begin{pmatrix} Y_2^{(6)} & Y_3^{(6)} & Y_1^{(6)} \\ Y_3^{(6)} & Y_1^{(6)} & Y_2^{(6)} \\ Y_1^{(6)} & Y_2^{(6)} & Y_3^{(6)} \end{pmatrix} + g_q \begin{pmatrix} Y_2'^{(6)} & Y_3'^{(6)} & Y_1'^{(6)} \\ Y_3'^{(6)} & Y_1'^{(6)} & Y_2'^{(6)} \\ Y_1'^{(6)} & Y_2'^{(6)} & Y_3'^{(6)} \end{pmatrix} \right]_{RL}, \quad (q = u \text{ or } d), \quad (38)$$

where $\hat{\alpha}_q \equiv \alpha_q/\gamma_q$ and $\hat{\beta}_q \equiv \beta_q/\gamma_q$. Then, we have three equations as:

$$\sum_{i=1}^3 m_{qi}^2 = \text{Tr}[M_q^\dagger M_q] = v_q^2 \gamma_q^2 (1 + \hat{\alpha}_q^2 + \hat{\beta}_q^2) C_1^q, \quad (39)$$

$$\prod_{i=1}^3 m_{qi}^2 = \text{Det}[M_q^\dagger M_q] = v_q^6 \gamma_q^6 \hat{\alpha}_q^2 \hat{\beta}_q^2 C_2^q, \quad (40)$$

$$\chi = \frac{\text{Tr}[M_q^\dagger M_q]^2 - \text{Tr}[(M_q^\dagger M_q)^2]}{2} = v_q^4 \gamma_q^4 (\hat{\alpha}_q^2 + \hat{\alpha}_q^2 \hat{\beta}_q^2 + \hat{\beta}_q^2) C_3^q, \quad (41)$$

where $\chi \equiv m_{q_1}^2 m_{q_2}^2 + m_{q_2}^2 m_{q_3}^2 + m_{q_3}^2 m_{q_1}^2$. The coefficients C_1^q , C_2^q , and C_3^q depend only on $Y_i^{(6)}$, $Y_i'^{(6)}$ and g_q , where $Y_i^{(6)}$ and $Y_i'^{(6)}$ are determined if the value of modulus τ is fixed, and g_q is an arbitrary complex coefficient. Those are given explicitly as follows:

$$\begin{aligned} C_1^q &= |\tilde{Y}_1|^2 + |\tilde{Y}_2|^2 + |\tilde{Y}_3|^2, \\ C_2^q &= |\tilde{Y}_1^3 + \tilde{Y}_2^3 + \tilde{Y}_3^3 - 3\tilde{Y}_1\tilde{Y}_2\tilde{Y}_3|^2, \\ C_3^q &= |\tilde{Y}_1|^4 + |\tilde{Y}_2|^4 + |\tilde{Y}_3|^4 + |\tilde{Y}_1\tilde{Y}_2|^2 + |\tilde{Y}_2\tilde{Y}_3|^2 + |\tilde{Y}_1\tilde{Y}_3|^2 - 2\text{Re} \left[\tilde{Y}_1^*\tilde{Y}_2^*\tilde{Y}_3^2 + \tilde{Y}_1^2\tilde{Y}_2^*\tilde{Y}_3^* + \tilde{Y}_1^*\tilde{Y}_2^2\tilde{Y}_3^* \right], \end{aligned}$$

where $\tilde{Y}_i \equiv Y_i^{(6)} + g_q Y_i'^{(6)}$ ($i = 1, 2, 3$).

Then, we obtain two equations which describe $\hat{\alpha}$ and $\hat{\beta}$ as forms of quark masses, τ and g_q :

$$\frac{(1+s)(s+t)}{t} = \frac{(\sum m_i^2/C_1^q)(\chi/C_3^q)}{\prod m_i^2/C_2^q}, \quad \frac{(1+s)^2}{s+t} = \frac{(\sum m_i^2/C_1^q)^2}{\chi/C_3^q}, \quad (42)$$

where we redefine the parameters $\hat{\alpha}_q^2 + \hat{\beta}_q^2 = s$ and $\hat{\alpha}_q^2 \hat{\beta}_q^2 = t$. They are related as follows:

$$\hat{\alpha}_q^2 = \frac{s \pm \sqrt{s^2 - 4t}}{2}, \quad \hat{\beta}_q^2 = \frac{s \mp \sqrt{s^2 - 4t}}{2}. \quad (43)$$

C Majorana and Dirac phases and $\langle m_{ee} \rangle$ in $0\nu\beta\beta$ decay

Supposing neutrinos to be Majorana particles, the PMNS matrix U_{PMNS} [61, 62] is parametrized in terms of the three mixing angles θ_{ij} ($i, j = 1, 2, 3$; $i < j$), one CP violating Dirac phase δ_{CP} and two Majorana phases α_{21} , α_{31} as follows:

$$U_{\text{PMNS}} = \begin{pmatrix} c_{12}c_{13} & s_{12}c_{13} & s_{13}e^{-i\delta_{\text{CP}}^\ell} \\ -s_{12}c_{23} - c_{12}s_{23}s_{13}e^{i\delta_{\text{CP}}^\ell} & c_{12}c_{23} - s_{12}s_{23}s_{13}e^{i\delta_{\text{CP}}^\ell} & s_{23}c_{13} \\ s_{12}s_{23} - c_{12}c_{23}s_{13}e^{i\delta_{\text{CP}}^\ell} & -c_{12}s_{23} - s_{12}c_{23}s_{13}e^{i\delta_{\text{CP}}^\ell} & c_{23}c_{13} \end{pmatrix} \begin{pmatrix} 1 & 0 & 0 \\ 0 & e^{i\frac{\alpha_{21}}{2}} & 0 \\ 0 & 0 & e^{i\frac{\alpha_{31}}{2}} \end{pmatrix}, \quad (44)$$

where c_{ij} and s_{ij} denote $\cos\theta_{ij}$ and $\sin\theta_{ij}$, respectively.

The rephasing invariant CP violating measure of leptons [65, 66] is defined by the PMNS matrix elements $U_{\alpha i}$. It is written in terms of the mixing angles and the CP violating phase as:

$$J_{CP} = \text{Im} [U_{e1}U_{\mu 2}U_{e2}^*U_{\mu 1}^*] = s_{23}c_{23}s_{12}c_{12}s_{13}c_{13}^2 \sin\delta_{\text{CP}}^\ell, \quad (45)$$

where $U_{\alpha i}$ denotes the each component of the PMNS matrix.

There are also other invariants I_1 and I_2 associated with Majorana phases

$$I_1 = \text{Im} [U_{e1}^*U_{e2}] = c_{12}s_{12}c_{13}^2 \sin\left(\frac{\alpha_{21}}{2}\right), \quad I_2 = \text{Im} [U_{e1}^*U_{e3}] = c_{12}s_{13}c_{13} \sin\left(\frac{\alpha_{31}}{2} - \delta_{\text{CP}}^\ell\right). \quad (46)$$

We can calculate δ_{CP}^ℓ , α_{21} and α_{31} with these relations by taking account of

$$\begin{aligned} \cos\delta_{CP}^\ell &= \frac{|U_{\tau 1}|^2 - s_{12}^2 s_{23}^2 - c_{12}^2 c_{23}^2 s_{13}^2}{2c_{12}s_{12}c_{23}s_{23}s_{13}}, \\ \text{Re} [U_{e1}^*U_{e2}] &= c_{12}s_{12}c_{13}^2 \cos\left(\frac{\alpha_{21}}{2}\right), \quad \text{Re} [U_{e1}^*U_{e3}] = c_{12}s_{13}c_{13} \cos\left(\frac{\alpha_{31}}{2} - \delta_{\text{CP}}^\ell\right). \end{aligned} \quad (47)$$

In terms of these parametrization, the effective mass for the $0\nu\beta\beta$ decay is given as follows:

$$\langle m_{ee} \rangle = \left| m_1 c_{12}^2 c_{13}^2 + m_2 s_{12}^2 c_{13}^2 e^{i\alpha_{21}} + m_3 s_{13}^2 e^{i(\alpha_{31} - 2\delta_{CP}^\ell)} \right|. \quad (48)$$

References

- [1] S. Pakvasa and H. Sugawara, Phys. Lett. **73B** (1978) 61.
- [2] F. Wilczek and A. Zee, Phys. Lett. **70B** (1977) 418 Erratum: [Phys. Lett. **72B** (1978) 504].
- [3] M. Fukugita, M. Tanimoto and T. Yanagida, Phys. Rev. D **57** (1998) 4429 [hep-ph/9709388].
- [4] Y. Fukuda *et al.* [Super-Kamiokande Collaboration], Phys. Rev. Lett. **81** (1998) 1562 [hep-ex/9807003].
- [5] G. Altarelli and F. Feruglio, Rev. Mod. Phys. **82** (2010) 2701 [arXiv:1002.0211 [hep-ph]].
- [6] H. Ishimori, T. Kobayashi, H. Ohki, Y. Shimizu, H. Okada and M. Tanimoto, Prog. Theor. Phys. Suppl. **183** (2010) 1 [arXiv:1003.3552 [hep-th]].
- [7] H. Ishimori, T. Kobayashi, H. Ohki, H. Okada, Y. Shimizu and M. Tanimoto, Lect. Notes Phys. **858** (2012) 1, Springer.
- [8] D. Hernandez and A. Y. Smirnov, Phys. Rev. D **86** (2012) 053014 [arXiv:1204.0445 [hep-ph]].
- [9] S. F. King and C. Luhn, Rept. Prog. Phys. **76** (2013) 056201 [arXiv:1301.1340 [hep-ph]].
- [10] S. F. King, A. Merle, S. Morisi, Y. Shimizu and M. Tanimoto, New J. Phys. **16**, 045018 (2014) [arXiv:1402.4271 [hep-ph]].
- [11] M. Tanimoto, AIP Conf. Proc. **1666** (2015) 120002.
- [12] S. F. King, Prog. Part. Nucl. Phys. **94** (2017) 217 [arXiv:1701.04413 [hep-ph]].
- [13] S. T. Petcov, Eur. Phys. J. C **78** (2018) no.9, 709 [arXiv:1711.10806 [hep-ph]].
- [14] E. Ma and G. Rajasekaran, Phys. Rev. D **64**, 113012 (2001) [arXiv:hep-ph/0106291].
- [15] K. S. Babu, E. Ma and J. W. F. Valle, Phys. Lett. B **552**, 207 (2003) [arXiv:hep-ph/0206292].
- [16] G. Altarelli and F. Feruglio, Nucl. Phys. B **720** (2005) 64 [hep-ph/0504165].
- [17] G. Altarelli and F. Feruglio, Nucl. Phys. B **741** (2006) 215 [hep-ph/0512103].
- [18] Y. Shimizu, M. Tanimoto and A. Watanabe, Prog. Theor. Phys. **126** (2011) 81 [arXiv:1105.2929 [hep-ph]].
- [19] S. T. Petcov and A. V. Titov, Phys. Rev. D **97** (2018) no.11, 115045 [arXiv:1804.00182 [hep-ph]].
- [20] S. K. Kang, Y. Shimizu, K. Takagi, S. Takahashi and M. Tanimoto, PTEP **2018**, no. 8, 083B01 (2018) [arXiv:1804.10468 [hep-ph]].
- [21] F. Feruglio, doi:10.1142/9789813238053-0012 arXiv:1706.08749 [hep-ph].
- [22] R. de Adelhart Toorop, F. Feruglio and C. Hagedorn, Nucl. Phys. B **858**, 437 (2012) [arXiv:1112.1340 [hep-ph]].

- [23] T. Kobayashi, K. Tanaka and T. H. Tatsuishi, Phys. Rev. D **98** (2018) no.1, 016004 [arXiv:1803.10391 [hep-ph]].
- [24] J. T. Penedo and S. T. Petcov, Nucl. Phys. B **939** (2019) 292 [arXiv:1806.11040 [hep-ph]].
- [25] P. P. Novichkov, J. T. Penedo, S. T. Petcov and A. V. Titov, JHEP **1904** (2019) 174 [arXiv:1812.02158 [hep-ph]].
- [26] J. C. Criado and F. Feruglio, SciPost Phys. **5** (2018) no.5, 042 [arXiv:1807.01125 [hep-ph]].
- [27] T. Kobayashi, N. Omoto, Y. Shimizu, K. Takagi, M. Tanimoto and T. H. Tatsuishi, JHEP **1811** (2018) 196 [arXiv:1808.03012 [hep-ph]].
- [28] P. P. Novichkov, J. T. Penedo, S. T. Petcov and A. V. Titov, JHEP **1904** (2019) 005 [arXiv:1811.04933 [hep-ph]].
- [29] T. Kobayashi, Y. Shimizu, K. Takagi, M. Tanimoto and T. H. Tatsuishi, arXiv:1907.09141 [hep-ph].
- [30] G. J. Ding, S. F. King and X. G. Liu, Phys. Rev. D **100** (2019) no.11, 115005 [arXiv:1903.12588 [hep-ph]].
- [31] X. G. Liu and G. J. Ding, JHEP **1908** (2019) 134 [arXiv:1907.01488 [hep-ph]].
- [32] F. J. de Anda, S. F. King and E. Perdomo, arXiv:1812.05620 [hep-ph].
- [33] P. P. Novichkov, S. T. Petcov and M. Tanimoto, Phys. Lett. B **793** (2019) 247 [arXiv:1812.11289 [hep-ph]].
- [34] T. Kobayashi and S. Tamba, Phys. Rev. D **99** (2019) no.4, 046001 [arXiv:1811.11384 [hep-th]].
- [35] A. Baur, H. P. Nilles, A. Trautner and P. K. S. Vaudrevange, Phys. Lett. B **795** (2019) 7 [arXiv:1901.03251 [hep-th]].
- [36] I. de Medeiros Varzielas, S. F. King and Y. L. Zhou, arXiv:1906.02208 [hep-ph].
- [37] P. P. Novichkov, J. T. Penedo, S. T. Petcov and A. V. Titov, JHEP **1907** (2019) 165 [arXiv:1905.11970 [hep-ph]].
- [38] T. Kobayashi, Y. Shimizu, K. Takagi, M. Tanimoto, T. H. Tatsuishi and H. Uchida, Phys. Lett. B **794** (2019) 114 [arXiv:1812.11072 [hep-ph]].
- [39] T. Kobayashi, Y. Shimizu, K. Takagi, M. Tanimoto and T. H. Tatsuishi, arXiv:1906.10341 [hep-ph].
- [40] H. Okada and M. Tanimoto, Phys. Lett. B **791** (2019) 54 [arXiv:1812.09677 [hep-ph]].
- [41] T. Nomura and H. Okada, Phys. Lett. B **797** (2019) 134799 [arXiv:1904.03937 [hep-ph]].
- [42] H. Okada and Y. Orikasa, arXiv:1907.04716 [hep-ph].

- [43] Y. Kariyazono, T. Kobayashi, S. Takada, S. Tamba and H. Uchida, Phys. Rev. D **100** (2019) no.4, 045014 [arXiv:1904.07546 [hep-th]].
- [44] K. Abe *et al.* [T2K Collaboration], Phys. Rev. Lett. **121** (2018) no.17, 171802 [arXiv:1807.07891 [hep-ex]].
- [45] P. Adamson *et al.* [NOvA Collaboration], Phys. Rev. Lett. **118** (2017) no.23, 231801 [arXiv:1703.03328 [hep-ex]].
- [46] J. Lauer, J. Mas and H. P. Nilles, Phys. Lett. B **226**, 251 (1989); Nucl. Phys. B **351**, 353 (1991).
- [47] W. Lerche, D. Lust and N. P. Warner, Phys. Lett. B **231**, 417 (1989).
- [48] S. Ferrara, D. Lust and S. Theisen, Phys. Lett. B **233**, 147 (1989).
- [49] D. Cremades, L. E. Ibanez and F. Marchesano, JHEP **0405**, 079 (2004) [hep-th/0404229].
- [50] T. Kobayashi and S. Nagamoto, Phys. Rev. D **96**, no. 9, 096011 (2017) [arXiv:1709.09784 [hep-th]].
- [51] T. Kobayashi, S. Nagamoto, S. Takada, S. Tamba and T. H. Tatsuishi, Phys. Rev. D **97**, no. 11, 116002 (2018) [arXiv:1804.06644 [hep-th]].
- [52] S. Ferrara, D. Lust, A. D. Shapere and S. Theisen, Phys. Lett. B **225**, 363 (1989).
- [53] M. C. Chen, S. Ramos-Sanchez and M. Ratz, arXiv:1909.06910 [hep-ph].
- [54] R. C. Gunning, *Lectures on Modular Forms* (Princeton University Press, Princeton, NJ, 1962).
- [55] B. Schoeneberg, *Elliptic Modular Functions* (Springer-Verlag, 1974).
- [56] N. Koblitz, *Introduction to Elliptic Curves and Modular Forms* (Springer-Verlag, 1984).
- [57] S. Antusch and V. Maurer, JHEP **1311** (2013) 115 [arXiv:1306.6879 [hep-ph]].
- [58] F. Björkeröth, F. J. de Anda, I. de Medeiros Varzielas and S. F. King, JHEP **1506** (2015) 141 [arXiv:1503.03306 [hep-ph]].
- [59] M. Tanabashi *et al.* [Particle Data Group], Phys. Rev. D **98** (2018) no.3, 030001.
- [60] I. Esteban, M. C. Gonzalez-Garcia, A. Hernandez-Cabezudo, M. Maltoni and T. Schwetz, JHEP **1901**, 106 (2019) [arXiv:1811.05487 [hep-ph]].
- [61] Z. Maki, M. Nakagawa and S. Sakata, Prog. Theor. Phys. **28** (1962) 870.
- [62] B. Pontecorvo, Sov. Phys. JETP **26** (1968) 984 [Zh. Eksp. Teor. Fiz. **53** (1967) 1717].
- [63] S. Vagnozzi, E. Giusarma, O. Mena, K. Freese, M. Gerbino, S. Ho and M. Lattanzi, Phys. Rev. D **96** (2017) no.12, 123503 [arXiv:1701.08172 [astro-ph.CO]].
- [64] N. Aghanim *et al.* [Planck Collaboration], arXiv:1807.06209 [astro-ph.CO].

- [65] C. Jarlskog, Phys. Rev. Lett. **55** (1985) 1039.
- [66] P. I. Krastev and S. T. Petcov, Phys. Lett. B **205** (1988) 84.